

## Spin-orbit coupling in nuclei and realistic nucleon-nucleon potentials

N. Kaiser

*Physik Department T39, Technische Universität München, D-85747 Garching, Germany*

(Received 28 April 2004; published 21 September 2004)

We analyze the spin-orbit coupling term in the nuclear energy density functional in terms of a zero-range NN-contact interaction and finite-range contributions from two-pion exchange. We show that the strength of the spin-orbit contact interaction as extracted from high-precision nucleon-nucleon potentials is in perfect agreement with that of phenomenological Skyrme forces employed in non-relativistic nuclear structure calculations. Additional long-range contributions from chiral two-pion exchange turn out to be relatively small. These explicitly density-dependent contributions reduce the ratio of the isovector to the isoscalar spin-orbit strength significantly below the Skyrme value 1/3. We perform a similar analysis for the strength function of the  $(\nabla\rho)^2$ -term and find values not far from those of phenomenological Skyrme parametrizations.

DOI: 10.1103/PhysRevC.70.034307

PACS number(s): 21.30.-x, 31.15.Ew

The microscopic understanding of the dynamical origin of the strong nuclear spin-orbit force is still one of the key problems in nuclear physics. The analogy to the spin-orbit interaction in atomic physics gave the hint that it could be a relativistic effect. This idea has led to the construction of the scalar-vector mean-field models for nuclear structure calculations [1,2]. In these models the nucleus is described as a collection of independent Dirac quasi-particles moving in self-consistently generated scalar and vector mean-fields. The footprints of relativity become visible through the large nuclear spin-orbit coupling which emerges in that framework naturally from the interplay of two strong and counteracting (scalar and vector) mean-fields. The corresponding many-body calculations are usually carried out in the Hartree approximation, ignoring exchange terms as well as the negative-energy Dirac-sea. The nucleon-nucleon interaction introduced into these models is to be considered as an effective one that is tailored to properties of finite nuclei but not constrained by the observables of free NN-scattering. For recent ideas about how the large Lorentz scalar and vector mean-fields can be linked to the condensate structure of the QCD-vacuum, see Ref. [3].

On the other hand phenomenological Skyrme forces have been (and still are) used extensively for the non-relativistic description of nuclei. In that approach the nuclear spin-orbit coupling is introduced by hand through a suitable NN-contact interaction (i.e., a spin-orbit delta-force) with an adjustable strength parameter  $W_0$ . Although there is a wide spread in the (other) parameters of the about one-hundred available Skyrme forces the one related to the spin-orbit coupling turns out to be rather stable with a value around  $W_0 \approx 120 \text{ MeV fm}^5$ . In fact one may even ignore the concept of an underlying effective (zero-range) two-body interaction and just take the emerging (parametrized) energy density functional as the true starting point for nuclear structure calculations within the self-consistent mean-field approximation. Such an interpretation is then in line with the energy functional approach to many-body problems of Kohn and Sham.

The more basic Dirac-Brueckner approach of Refs. [4,5] solves a relativistically improved Bethe-Goldstone equation with a realistic nucleon-nucleon interaction parametrized in

terms of one-boson exchange potentials. This Lorentz-covariant approach is able to describe properties of nuclear matter and finite nuclei without any new adjustable parameter. In particular, the spin-orbit splittings of medium and heavy nuclei are correctly reproduced (in local density approximation). A drawback of the method is that the underlying NN-interaction has been constructed without the explicit use of chiral symmetry. In a relativistic Hartree-description there is a close connection between the mean-field potential and the spin-orbit one, since they differ only by the sign of the vector-meson exchange contribution, while in non-relativistic approaches there is no connection at all. Unfortunately there is no direct experimental hint for either possibility. Despite all its known successes the fully relativistic treatment of the nuclear many-body problem seems unnatural in view of the small ratio  $(k_{f0}/M)^2 \approx 0.08$ , with  $k_{f0} \approx 263 \text{ MeV}$  the Fermi momentum of equilibrated nuclear matter and  $M=939 \text{ MeV}$  the (free) nucleon mass.

The purpose of the present paper is to show that the spin-orbit interaction relevant for the structure of (medium and heavy) nuclei is quantitatively consistent with that relevant for low-energy elastic NN-scattering. We demonstrate that the short-range spin-orbit interaction as extracted from various high-precision nucleon-nucleon potentials (which accurately fit all NN-phase shifts and mixing angles below the NN $\pi$ -threshold) is in perfect agreement with the one needed in non-relativistic nuclear structure calculations (using the Skyrme phenomenology). Additional long-range spin-orbit couplings generated by chiral two-pion exchange turn out to be relatively small. These explicitly density dependent effects reduce favorably the ratio of the isovector to the isoscalar spin-orbit coupling strength. We perform also a similar analysis of the  $(\nabla\rho)^2$ -term and find reasonable values for its strength function (at densities  $\rho > 0.05 \text{ fm}^{-3}$ ).

Let us begin by writing down the explicit form of the spin-orbit coupling term in the nuclear energy density functional:

$$\mathcal{E}_{\text{so}}[\rho_p, \rho_n, \mathbf{J}_p, \mathbf{J}_n] = F_{\text{so}}(k_f) \nabla\rho \cdot \mathbf{J} + G_{\text{so}}(k_f) \nabla\rho_v \cdot \mathbf{J}_v, \quad (1)$$

where the sums  $\rho = \rho_p + \rho_n$ ,  $\mathbf{J} = \mathbf{J}_p + \mathbf{J}_n$  and differences  $\rho_v = \rho_p - \rho_n$ ,  $\mathbf{J}_v = \mathbf{J}_p - \mathbf{J}_n$  of proton and neutron quantities have been introduced,

$$\rho_{p,n}(\mathbf{r}) = \frac{k_{p,n}^3(\mathbf{r})}{3\pi^2} = \sum_{\alpha \in \text{occ}} \Psi_{p,n}^{(\alpha)\dagger}(\mathbf{r}) \Psi_{p,n}^{(\alpha)}(\mathbf{r}), \quad (2)$$

denote the local proton and neutron densities which we have rewritten in terms of the corresponding (local) proton and neutron Fermi-momenta  $k_{p,n}(\mathbf{r})$  and expressed as sums over the occupied single-particle orbitals  $\Psi_{p,n}^{(\alpha)}(\mathbf{r})$ . The spin-orbit densities of the protons and neutrons are defined similarly:

$$\mathbf{J}_{p,n}(\mathbf{r}) = \sum_{\alpha \in \text{occ}} \Psi_{p,n}^{(\alpha)\dagger}(\mathbf{r}) i\boldsymbol{\sigma} \times \nabla \Psi_{p,n}^{(\alpha)}(\mathbf{r}). \quad (3)$$

Furthermore,  $F_{\text{so}}(k_f)$  and  $G_{\text{so}}(k_f)$  in Eq. (1) denote the density dependent isoscalar and isovector spin-orbit strength functions. In Skyrme parametrizations [6] these are density-independent constants,  $F_{\text{so}}(k_f) = 3G_{\text{so}}(k_f) = 3W_0/4 \approx 90 \text{ MeV fm}^5$ , determined by one single spin-orbit force parameter  $W_0$ .

The starting point for the construction of an explicit nuclear energy density functional  $\mathcal{E}_{\text{sol}}[\rho_p, \rho_n, \mathbf{J}_p, \mathbf{J}_n]$  is the bilocal density-matrix as given by a sum over the occupied energy eigenfunctions:  $\sum_{\alpha \in \text{occ}} \Psi_{p,n}^{(\alpha)}(\mathbf{r}-\mathbf{a}/2) \Psi_{p,n}^{(\alpha)\dagger}(\mathbf{r}+\mathbf{a}/2)$ . According to Negele and Vautherin [7] it can be expanded in relative and center-of-mass coordinates,  $\mathbf{a}$  and  $\mathbf{r}$ , with expansion coefficients determined by purely local quantities (nucleon density, kinetic energy density and spin-orbit density). As outlined in Sec. 2 of Ref. [8] the Fourier-transform of the (so expanded) density-matrix defines in momentum-space a medium-insertion for the inhomogeneous many-nucleon system. It is straightforward to generalize this construction to the isospin-asymmetric situation of different proton and neutron local densities,  $\rho_{p,n}(\mathbf{r})$  and  $\mathbf{J}_{p,n}(\mathbf{r})$ . We display here only that part of the medium-insertion  $\Gamma(\mathbf{p}, \mathbf{q})$  which is actually relevant for the diagrammatic calculation of the isoscalar and isovector spin-orbit terms defined in Eq. (1):

$$\begin{aligned} \Gamma(\mathbf{p}, \mathbf{q}) = & \int d^3r e^{-i\mathbf{q}\cdot\mathbf{r}} \left\{ \frac{1+\tau_3}{2} \theta(k_p - |\mathbf{p}|) + \frac{1-\tau_3}{2} \theta(k_n - |\mathbf{p}|) \right. \\ & + \frac{\pi^2}{4k_f^4} [\delta(k_f - |\mathbf{p}|) - k_f \delta'(k_f - |\mathbf{p}|)] \\ & \left. \times (\boldsymbol{\sigma} \times \mathbf{p}) \cdot (\mathbf{J} + \tau_3 \mathbf{J}_v) \right\}. \quad (4) \end{aligned}$$

The double line in Fig. 1 symbolizes this medium insertion together with the assignment of the out- and in-going nucleon momenta  $\mathbf{p} \pm \mathbf{q}/2$ . The momentum transfer  $\mathbf{q}$  is provided by the Fourier components of the inhomogeneous matter distributions  $\rho_{p,n}(\mathbf{r})$  and  $\mathbf{J}_{p,n}(\mathbf{r})$ .

Next, we write down the lowest order four-nucleon contact-coupling which generates a spin-orbit interaction:

$$\begin{aligned} \mathcal{L}_{NN}^{(\text{so})} = & -i \frac{C_5}{8} \{ (N^\dagger \nabla N) \cdot (\nabla N^\dagger \times \boldsymbol{\sigma} N) \\ & + (\nabla N^\dagger N) \cdot (N^\dagger \boldsymbol{\sigma} \times \nabla N) - (N^\dagger N) (\nabla N^\dagger \cdot \boldsymbol{\sigma} \times \nabla N) \\ & + (N^\dagger \boldsymbol{\sigma} N) \cdot (\nabla N^\dagger \times \nabla N) \}. \quad (5) \end{aligned}$$

This Lagrangian, together with the notation  $C_5$  for the cou-

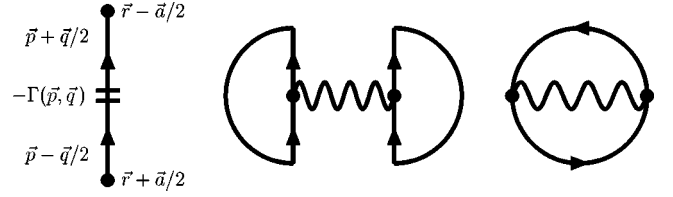


FIG. 1. Left: The double line symbolizes the medium insertion  $\Gamma(\mathbf{p}, \mathbf{q})$  defined by Eq. (4). Next shown are generic two-body Hartree and Fock diagrams. Their combinatoric factor is  $1/2$ . The wiggly line symbolizes the spin-orbit NN-interaction.

pling constant, has been taken over from Ref. [9]. The somewhat lengthy expression in Eq. (5) is dictated by Galilei invariance as will become clear immediately. The contribution of the contact-Lagrangian  $\mathcal{L}_{NN}^{(\text{so})}$  to the T-matrix of the scattering process  $N(\mathbf{p}_1) + N(\mathbf{p}_2) \rightarrow N(\mathbf{p}'_1) + N(\mathbf{p}'_2)$  reads:

$$\begin{aligned} & -i \frac{C_5}{8} (\boldsymbol{\sigma}_1 + \boldsymbol{\sigma}_2) \cdot [(\mathbf{p}'_1 - \mathbf{p}'_2) \times (\mathbf{p}_1 - \mathbf{p}_2)] \\ & = -i \frac{C_5}{4} (\boldsymbol{\sigma}_1 + \boldsymbol{\sigma}_2) \cdot [(\mathbf{p}'_1 - \mathbf{p}_1) \times (\mathbf{p}_1 - \mathbf{p}_2)], \quad (6) \end{aligned}$$

where Galilei invariance is now manifest, since only differences of momenta occur.  $\boldsymbol{\sigma}_{1,2}$  denote the conventional spin-operators of the two nucleons. Furthermore, by comparing with the analogous T-matrix element of the Skyrme spin-orbit interaction proportional to  $W_0$  (see Eq. (4.105) in Ref. [10]) one finds the relation  $C_5 = 2W_0$  between coupling parameters. As a side remark we note that the spin-orbit term which arises from heavy scalar and vector boson exchange between nucleons has the property of Galilei invariance only if the respective ratios of mass to coupling constant are equal:  $m_S/g_S = m_V/g_V$ . The corresponding contribution to the strength parameter  $C_5$  reads in that case:  $C_5^{(S+V)} = 2(1 + \kappa_V)(g_V/Mm_V)^2$  where  $M = 939 \text{ MeV}$  stands for (average) the nucleon mass and  $\kappa_V$  denotes the tensor-to-vector coupling ratio of the heavy vector boson (e.g. the  $\omega(782)$ -meson).

In the work of Epelbaum *et al.* [9] numerical values are given for the so-called spectroscopic low-energy constants which characterize the short-range part of the nucleon-nucleon potential in certain low partial waves (S- and P-waves). The spin-orbit strength parameter  $C_5 = 2W_0$  of interest here is determined by the following linear combination of the  $^3P$ -wave low-energy constants:

$$C_5 = \frac{1}{16\pi} [2C(^3P_0) + 3C(^3P_1) - 5C(^3P_2)]. \quad (7)$$

This simple relation is central to our work since it allows one to connect the phenomenological Skyrme parameter  $W_0 = C_5/2$  with the low-energy dynamics of elastic NN-scattering.

We continue with the general form of the spin-orbit part in the NN T-matrix (using the sign-convention of Ref. [11]). For the scattering process  $N(\mathbf{p}) + N(-\mathbf{p}) \rightarrow N(\mathbf{p} + \mathbf{q}) + N(-\mathbf{p} - \mathbf{q})$  in the center-of-mass frame it reads:

TABLE I. Numerical values of the spin-orbit strength parameter  $3W_0/4$  for various phenomenological Skyrme forces.

Skyrme force	SIII	SkM	SkP	Sly4-7	MSk1-6	SkI1-5
$3W_0/4$ [MeV fm <sup>5</sup> ]	90.0	97.5	75.0	93.2	87.6	92.7

$$\mathcal{T}_{NN}^{(\text{so})} = [V_{\text{so}}(q) + \boldsymbol{\tau}_1 \cdot \boldsymbol{\tau}_2 W_{\text{so}}(q)] i(\boldsymbol{\sigma}_1 + \boldsymbol{\sigma}_2) \cdot (\mathbf{q} \times \mathbf{p}). \quad (8)$$

Here,  $\mathbf{q}$  is the momentum transfer between both nucleons and  $V_{\text{so}}(q)$  and  $W_{\text{so}}(q)$  denote the isoscalar and isovector spin-orbit NN-amplitudes, respectively. With the help of the medium insertion  $\Gamma(\mathbf{p}, \mathbf{q})$  in Eq. (4) one can now calculate diagrammatically the nuclear energy density functional  $\mathcal{E}_{\text{so}}[\rho_p, \rho_n, \mathbf{J}_p, \mathbf{J}_n]$ . From the Hartree and Fock diagrams in Fig. 1 one obtains the following formulas for two-body contributions to the isoscalar and isovector spin-orbit strength functions:

$$F_{\text{so}}(k_f)^{(\text{two-body})} = -\frac{1}{6} \left\{ 3V_{\text{so}}(0) + V_{\text{so}}(2k_f) + 3W_{\text{so}}(2k_f) + \int_0^1 dx x [V_{\text{so}}(2xk_f) + 3W_{\text{so}}(2xk_f)] \right\}, \quad (9)$$

$$G_{\text{so}}(k_f)^{(\text{two-body})} = \frac{1}{6} \left\{ W_{\text{so}}(2k_f) - V_{\text{so}}(2k_f) - 3W_{\text{so}}(0) + \int_0^1 dx x [W_{\text{so}}(2xk_f) - V_{\text{so}}(2xk_f)] \right\}. \quad (10)$$

Here, the terms  $-V_{\text{so}}(0)/2$  and  $-W_{\text{so}}(0)/2$  belong to the Hartree diagram (with two closed nucleon lines) while the remaining ones summarize the contribution from the Fock diagram (having just one closed nucleon line). After the obvious identification  $V_{\text{so}}(q)^{(\text{ct})} = -C_5/2$  [compare Eq. (6) with Eq. (8)] one derives the following contribution of the four-nucleon contact-vertex to the spin-orbit strength functions:

$$F_{\text{so}}(k_f)^{(\text{ct})} = \frac{3C_5}{8}, \quad G_{\text{so}}(k_f)^{(\text{ct})} = \frac{C_5}{8}. \quad (11)$$

The fixed ratio of isovector-to-isoscalar spin-orbit strength  $G_{\text{so}}(k_f)/F_{\text{so}}(k_f) = 1/3$  is a consequence of the Pauli exclusion principle for a zero-range spin-orbit interaction.

The long-range contributions to the spin-orbit NN-potential arise naturally from two-pion exchange between nucleons in the form of a relativistic  $1/M$ -correction. The corresponding lowest order  $2\pi$ -exchange triangle and box

diagrams have been evaluated in Sec. 4.2 of Ref. [11]. Inserting the corresponding analytical expressions for  $V_{\text{so}}(q)$  and  $W_{\text{so}}(q)$  [see Eqs. (22,23) in Ref. [11]] into the master formulas (9) and (10) one gets the following contributions from chiral  $2\pi$ -exchange to the spin-orbit strength functions:

$$F_{\text{so}}(k_f)^{(2\pi)} = \frac{g_A^2 m_\pi}{\pi M (4f_\pi)^4} \left\{ \frac{10}{3} - \frac{3g_A^2}{2} + \frac{4-3g_A^2}{6u^2} \ln(1+u^2) + \left[ \frac{2}{u}(g_A^2-2) - \frac{8u}{3} \right] \arctan u \right\}, \quad (12)$$

$$G_{\text{so}}(k_f)^{(2\pi)} = \frac{g_A^2 m_\pi}{9\pi M (4f_\pi)^4} \left\{ \frac{53g_A^2}{2} - 10 + \frac{7g_A^2-4}{2u^2} \ln(1+u^2) + \left[ \frac{6}{u}(2-5g_A^2) + 8u(1-4g_A^2) \right] \arctan u \right\}, \quad (13)$$

with the abbreviation  $u = k_f/m_\pi$  where  $m_\pi = 135$  MeV stands for the (neutral) pion mass. As usual  $f_\pi = 92.4$  MeV denotes the weak pion decay constant and we choose the value  $g_A = 1.3$  for the nucleon axial vector coupling constant. Note that we have normalized the density dependent expressions in Eqs. (12) and (13) to the value zero at zero density ( $k_f = 0$ ). This way one eliminates automatically all (regularization dependent) short-range contributions which conceptually belong to the low-energy constant  $C_5$ . As stressed in Ref. [9] such a separation of long and short-distance dynamics is necessary in order to be able to compare with results extracted from realistic NN-potentials. At the next order in the small momentum expansion there are  $2\pi$ -exchange diagrams with one chiral  $\pi\pi NN$ -contact vertex. The corresponding spin-orbit NN-amplitudes have been written down in Eqs. (13), (15), and (16) of Ref. [12]. After performing the necessary integration and subtraction at  $k_f = 0$  one gets the following  $2\pi$ -exchange contributions to the spin-orbit strength functions:

 TABLE II. Numerical values of the short-range spin-orbit strength parameter  $3C_5/8$  for various nucleon-nucleon potentials. The so-called high-precision potentials are marked by an asterisk.

NN-potential	Bonn-B	CD-Bonn*	Nijm-93	Nijm-I	Nijm-II*	AV-18*	NNLO
$3C_5/8$ [MeV fm <sup>5</sup> ]	80.3	89.6	79.9	82.4	87.7	88.9	73...92

$$\begin{aligned}
F_{\text{so}}(k_f)^{(2\pi-c_j)} = & \frac{m_\pi^2}{3\pi^2 M (4f_\pi)^4} \left\{ 20u^2 [c_4 + g_A^2(5c_4 - 2c_2)] \ln \frac{m_\pi}{\Lambda} \right. \\
& - 29c_4 + g_A^2(58c_2 - 61c_4) + u^2 [g_A^2(2c_2 - 5c_4) \\
& - c_4] + \left[ \frac{2}{u} (13c_4 + g_A^2(29c_4 - 26c_2)) + 20u(c_4 \right. \\
& \left. + g_A^2(5c_4 - 2c_2)) \right] \sqrt{1+u^2} \ln(u + \sqrt{1+u^2}) \\
& \left. + \frac{3}{u^2} [c_4 + g_A^2(c_4 - 2c_2)] \ln^2(u + \sqrt{1+u^2}) \right\}, \quad (14)
\end{aligned}$$

$$\begin{aligned}
G_{\text{so}}(k_f)^{(2\pi-c_j)} = & \frac{m_\pi^2}{9\pi^2 M (4f_\pi)^4} \left\{ -20u^2 [c_4 + g_A^2(5c_4 \right. \\
& \left. + 6c_2)] \ln \frac{m_\pi}{\Lambda} + 29c_4 + g_A^2(174c_2 + 61c_4) \right. \\
& \left. + u^2 [c_4 + g_A^2(6c_2 + 5c_4)] - \left[ \frac{2}{u} (13c_4 + g_A^2(78c_2 \right. \right. \\
& \left. \left. + 29c_4)) + 20u(c_4 + g_A^2(5c_4 + 6c_2)) \right] \sqrt{1+u^2} \right. \\
& \left. \times \ln(u + \sqrt{1+u^2}) - \frac{3}{u^2} [c_4 + g_A^2(c_4 + 6c_2)] \right. \\
& \left. \times \ln^2(u + \sqrt{1+u^2}) \right\}. \quad (15)
\end{aligned}$$

The two occurring low-energy constants  $c_2=3.2 \text{ GeV}^{-1}$  and  $c_4=3.4 \text{ GeV}^{-1}$  [13] represent mainly effects from (single) virtual  $\Delta(1232)$ -isobar excitation. In these expressions we have also introduced  $k_f^2$ -terms proportional to the chiral logarithm  $\ln(m_\pi/\Lambda)$  in order to guarantee finite results for  $F_{\text{so}}(k_f)^{(2\pi-c_j)}$  and  $G_{\text{so}}(k_f)^{(2\pi-c_j)}$  in the strict chiral limit  $m_\pi=0$ .

Now we can turn to numerical results. In Table I we have collected values for the isoscalar spin-orbit strength  $3W_0/4$  of various phenomenological Skyrme forces, SIII [14], SkM [15], SkP [16], Sly [17], MSk [18] and SkI [19]. In the cases of Sly, MSk and SkI we have performed averages over several (slightly different) parameter sets Sly4-7, MSk1-6 and SkI1-5. One sees that the entries in Table I scatter somewhat around a mean value of about  $3W_0/4 \approx 90 \text{ MeV fm}^5$ , which can therefore be considered as the empirical spin-orbit strength relevant for nuclear structure. In Table II we give the equivalent spin-orbit strength parameter  $3C_5/8$  as extracted from various realistic nucleon-nucleon potentials. These numbers have been produced with the help of Table IV in Ref. [9] by forming the appropriate linear combination Eq. (7) of  $C(^3P_{0,1,2})$ . The last entry "NNLO" in Table II corresponds to the chiral NN-potential of Epelbaum *et al.* [9] where the cut-off  $\Lambda$  has been varied between 0.5 and

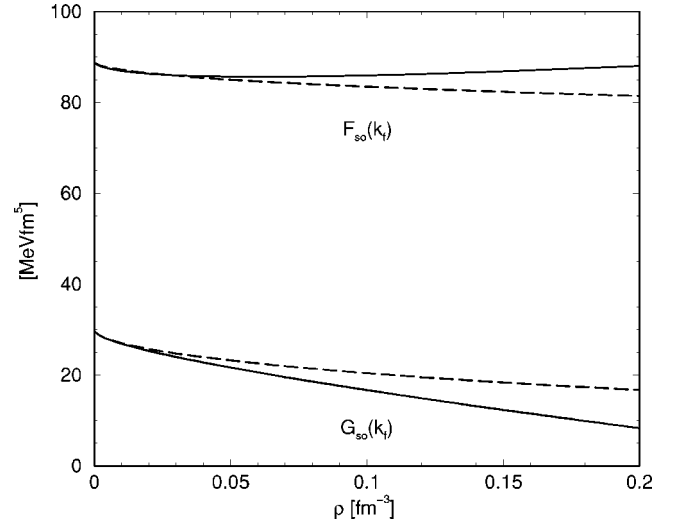


FIG. 2. The isoscalar and isovector spin-orbit strength functions  $F_{\text{so}}(k_f)$  and  $G_{\text{so}}(k_f)$  versus the nucleon density  $\rho=2k_f^3/3\pi^2$ . The dashed curves show the result of the spin-orbit contact-coupling  $C_5$  and irreducible two-pion exchange Eqs. (12) and (13). The full curves include in addition the two-pion exchange contributions Eqs. (14) and (15) proportional to  $c_{2,4}$ . The scale in the chiral logarithm is chosen as  $\Lambda=0.5 \text{ GeV}$ .

0.6 GeV (see Table I in Ref. [5]). It is astonishing to observe that these realistic NN-potentials which are essentially adjusted to empirical low-energy NN-scattering data give numbers close to those of the phenomenological Skyrme forces. This holds in particular for the so-called high-precision NN-potentials CD-Bonn [20], Nijm-II [21] and AV-18 [22] (marked by an asterisk in Table II) where  $3C_5/8$  comes out very close to  $3C_5/8 \approx 90 \text{ MeV fm}^5$ . Therefore one can conclude that the strength of the spin-orbit interaction necessary for nuclear structure is perfectly consistent with that needed to describe low-energy NN-scattering data. This observation is the one of the main results of the present work.

The recently constructed universal low-momentum nucleon-nucleon potential  $V_{\text{low-k}}$  offers another possibility to extract the short-range spin-orbit parameter  $3C_5/8$ . From the curvatures of the (diagonal)  $^3P$ -wave potentials shown in Figs. 4, 18 of Ref. [23] we get after multiplying the relevant linear combination  $2(^3P_0) + 3(^3P_1) - 5(^3P_2)$  with the conversion factor  $3\pi/8M$  the value  $3C_5/8=79 \text{ MeV fm}^5$  from  $V_{\text{low-k}}$ . This somewhat smaller value (in comparison to the high-precision potentials) finds its explanation in the fact that the "full" NN-potential and  $V_{\text{low-k}}$  differ by some local contact-terms [24]. Indeed the numerical values of the counter-terms listed in Table 1 of Ref. [24] give rise to an additional contribution to  $3C_5/8$  of  $10.4 \text{ MeV fm}^5$  which then closes the gap to the empirical value of  $3C_5/8 \approx 90 \text{ MeV fm}^5$ .

In Fig. 2 we show the isoscalar and isovector spin-orbit strength functions  $F_{\text{so}}(k_f)$  and  $G_{\text{so}}(k_f)$  as a function of the nucleon density  $\rho=2k_f^3/3\pi^2$ . The dashed lines result from the average value  $3C_5/8=88.7 \text{ MeV fm}^5$  of the three high-precision NN-potentials and the lowest order irreducible

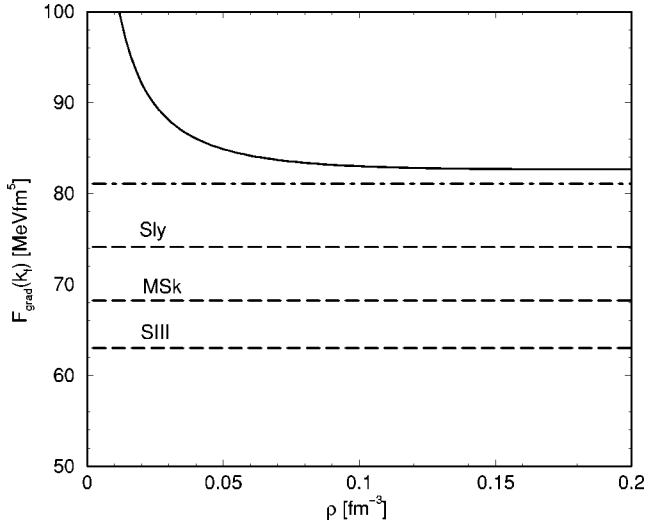


FIG. 3. The strength function  $F_{\nabla}(k_f)$  related to the  $(\nabla\rho)^2$ -term in the nuclear energy density functional versus the nucleon density  $\rho = 2k_f^3/3\pi^2$ . The three horizontal dashed lines show the constant values  $F_{\nabla}(k_f) = [9t_1 - (5+4x_2)t_2]/64$  of the Skyrme forces Sly [17], MSk [18] and SIII [14]. The dashed-dotted line gives the mean value  $F_{\nabla}(k_f)^{(ct)} = 81.1 \text{ MeV fm}^5$  of the three high-precision NN-potentials CD-Bonn, Nijm-II, and AV-18. The full line includes in addition the  $1\pi$ - and  $2\pi$ -exchange contributions Eqs. (18) and (19).

$2\pi$ -exchange contributions Eqs. (12) and (13). The full lines include in addition the next-to-leading order  $2\pi$ -exchange contributions proportional to the low-energy constants  $c_2 = 3.2 \text{ GeV}^{-1}$  and  $c_4 = 3.4 \text{ GeV}^{-1}$  [13]. The scale  $\Lambda$  in the chiral logarithm  $\ln(m_\pi/\Lambda)$  has been chosen equal to the momentum cut-off  $\Lambda = 0.5 \text{ GeV}$  of Ref. [9]. In the case of the isoscalar spin-orbit strength function  $F_{so}(k_f)$  one finds that the two-pion exchange effects are relatively small and that they also cancel each other to a large extent. In contrast to this behavior the isovector spin-orbit strength function  $G_{so}(k_f)$  gets reduced with increasing density. At nuclear matter saturation density  $\rho_0 \approx 0.16 \text{ fm}^{-3}$  the ratio  $G_{so}(k_{f0})/F_{so}(k_{f0})$  is about 1/8, substantially less than the Skyrme value 1/3. As pointed out in Ref. [19] such a reduction of the isovector spin-orbit mean-field (proportional to  $\nabla\rho_n - \nabla\rho_p$ ) is favorable for an accurate description of isotope shifts in the Pb region. It seems that the isospin dependence of the spin-orbit interaction is a property for which two-pion exchange induced effects can play a role in nuclear structure.

For the sake of completeness we also note that even the one-pion exchange Fock diagram gives rise to non-vanishing spin-orbit strength functions:

$$F_{so}(k_f)^{(1\pi)} = -3G_{so}(k_f)^{(1\pi)} = \frac{g_A^2}{(16Mf_\pi)^2} [u^{-2} \ln(1+4u^2) - 4]. \quad (16)$$

In order to arrive at this result one has to expand the relativistic pseudovector  $\pi NN$ -vertex up to order  $1/M^2$ . As expected the  $1\pi$ -exchange contributions to the spin-orbit strengths are negligibly small. For example, at a density of  $\rho_0/2 \approx 0.08 \text{ fm}^{-3}$  one gets  $F_{so}^{(1\pi)}(k_f) \approx -0.79 \text{ MeV fm}^5$  which

corresponds in magnitude to less than 1% of the empirical value  $90 \text{ MeV fm}^5$ .

Finally, we perform the same analysis for the  $(\nabla\rho)^2$ -term in the nuclear energy density functional:  $F_{\nabla}(k_f)(\nabla\rho)^2$ . Its strength function  $F_{\nabla}(k_f)$  is also decomposed into contributions from zero-range NN-contact interactions and long-range one- and two-pion exchange. From the complete set of four-nucleon contact-couplings written down in Ref. [9] one gets:

$$\begin{aligned} F_{\nabla}(k_f)^{(ct)} &= \frac{1}{32}(14C_1 + C_2 - 6C_3 - 3C_4 - 2C_6 - C_7) \\ &= \frac{3}{512\pi} [6C(^1S_0) + 6C(^3S_1) - C(^1P_1) - C(^3P_0) \\ &\quad - 3C(^3P_1) - 5C(^3P_2)], \end{aligned} \quad (17)$$

where we have reexpressed the relevant linear combination of  $C_1, \dots, C_7$  through the so-called spectroscopic low-energy constants. In that representation we obtain from the entries in Table IV of Ref. [9] for the three high-precision NN-potentials CD-Bonn, Nijm-II and AV-18 the values  $F_{\nabla}^{(ct)}(k_f) = 82.4 \text{ MeV fm}^5$ ,  $78.4 \text{ MeV fm}^5$  and  $82.5 \text{ MeV fm}^5$ , respectively. The contribution of the one-pion exchange Fock diagram to the strength function  $F_{\nabla}(k_f)$  reads on the other hand [8]:

$$\begin{aligned} F_{\nabla}(k_f)^{(1\pi)} &= \frac{35g_A^2 u^{-7}}{(16m_\pi f_\pi)^2} \left\{ \frac{7}{8u} - \frac{21u}{2} - \frac{u^3}{6} \right. \\ &\quad + \frac{72u^4 - 90u^2 - 7}{32u^3} \ln(1+4u^2) + 10 \arctan 2u \\ &\quad + \frac{m_\pi^2}{16M^2} \left[ \frac{3}{4u} + \frac{193u}{2} - 12u^3 + \frac{4u^5}{3} - \frac{96u^7}{35} \right. \\ &\quad + 20(2u^2 - 3) \arctan 2u + \left. \left. \left( \frac{11}{2u} - 45u - \frac{3}{16u^3} \right) \ln(1+4u^2) \right] \right\}, \end{aligned} \quad (18)$$

where we have included also the relativistic  $1/M^2$ -correction. The contributions of (lowest order) irreducible  $2\pi$ -exchange to the NN-potential have been evaluated in Ref. [11] [see Eqs. (14,15) therein]. Application of the density-matrix expansion of Negele and Vautherin [7] as outlined in Sec. 2 of Ref. [8] leads then to the following contribution of irreducible  $2\pi$ -exchange to the strength function  $F_{\nabla}(k_f)$ :

$$\begin{aligned}
F_{\nabla}(k_f)^{(2\pi)} = \frac{u^{-10}}{\pi^2(16f_\pi)^4} & \left\{ [245(71g_A^4 + 10g_A^2 - 1) + 1575u^2(43g_A^4 + 6g_A^2 - 1) - 840u^4(23g_A^4 + 2g_A^2 - 1)] \ln^2(u + \sqrt{1+u^2}) + \frac{2u}{3} \right. \\
& \times \sqrt{1+u^2} \ln(u + \sqrt{1+u^2}) [735(1 - 10g_A^2 - 71g_A^4) + 5u^2(31859g_A^4 + 3502g_A^2 - 1201) + 2u^4(869g_A^4 - 230g_A^2 - 79) \\
& + 24u^6(2u^2 - 1)(11g_A^4 - 10g_A^2 - 1)] + 245u^2(71g_A^4 + 10g_A^2 - 1) - \frac{20u^4}{3}(23479g_A^4 + 2801g_A^2 - 800) + \frac{u^6}{3}(551 + 470g_A^2 \\
& \left. - 7181g_A^4) + 4u^8(27g_A^4 - 22g_A^2 - 5) + \frac{4u^{10}}{105}(869 + 7010g_A^2 - 6199g_A^4) \right\}. \quad (19)
\end{aligned}$$

Again, in order to have a clean separation between (regularization dependent) short-distance effects and genuine long-distance contributions we have normalized this expression to  $F_{\nabla}(0)^{(2\pi)}=0$ .

In Fig. 3 we show the strength function  $F_{\nabla}(k_f)$  versus the nucleon density  $\rho=2k_f^3/3\pi^2$ . The three horizontal dashed lines represent the constant values  $F_{\nabla}(k_f)=[9t_1-(5+4x_2)t_2]/64$  of the Skyrme forces Sly [17], MSk [18] and SIII [14]. The dashed-dotted line gives the mean value  $F_{\nabla}(k_f)^{(ct)}=81.1$  MeV fm<sup>5</sup> of the three high precision potentials CD-Bonn, Nijm-II and AV-18. The full line includes in addition the  $1\pi$ - and  $2\pi$ -exchange contributions Eqs. (18) and (19). One observes a rough agreement between these different curves. For densities  $\rho>0.05$  fm<sup>-3</sup> our prediction for  $F_{\nabla}(k_f)$  exceeds the mean value of the phenomenological Sly4-7 forces [17] only by about 15%. Below that density, however, a strong rise of the strength function  $F_{\nabla}(k_f)$  sets in. This behavior originates from the static  $1\pi$ -exchange contribution with its inherent chiral singularity  $m_\pi^{-2}$  which becomes dominant at extremely low densities  $k_f \ll m_\pi/2$  [8]. Our derivation of the strength function  $F_{\nabla}(k_f)$  is based on the density-matrix expansion of Negele and Vautherin, [7] which has been found to become inaccurate for low and nonuniform densities [25]. Therefore one should not trust the full line in

Fig. 3 below  $\rho \leq \rho_0/4 \simeq 0.04$  fm<sup>-3</sup>. It is also evident from Fig. 3 that the nuclear structure phenomenology does presently not constrain the  $(\nabla\rho)^2$ -term as strongly as the spin-orbit coupling term. The existing Skyrme forces show an appreciable variation of the associated strength parameter.

In summary, we analyzed in this work the spin-orbit coupling term in the nuclear energy density functional in terms of a zero-range NN-contact interaction and finite-range contributions from chiral two-pion exchange. We have shown that the strength of the spin-orbit contact-interaction as extracted from high-precision NN-potentials agrees perfectly with that of phenomenological Skyrme forces employed in non-relativistic nuclear structure calculations. The numerical results collected in Table IV of Ref. [9] have been essential in order to establish this fact. Additional long-range effects from chiral two-pion exchange seem to play a role for the isospin dependence of the spin-orbit coupling. The ratio of the isovector to the isoscalar spin-orbit strength gets significantly reduced below the Skyrme value 1/3. Such a reduction is favorable for an accurate description of the isotope shifts in Pb nuclei [19]. Furthermore, we have performed the same analysis for the strength function of the  $(\nabla\rho)^2$ -term and found values not far from those of phenomenological Skyrme parametrizations.

- 
- [1] B.D. Serot and J.D. Walecka, *Int. J. Mod. Phys. E* **6**, 515 (1997), and references therein.
- [2] P. Ring, *Prog. Part. Nucl. Phys.* **37**, 193 (1996), and references therein.
- [3] P. Finelli, N. Kaiser, D. Vretenar, and W. Weise, *Eur. Phys. J. A* **17**, 573 (2003); *Nucl. Phys.* **A735**, 449 (2004).
- [4] R. Brockmann and R. Machleidt, in *International Review of Nuclear Physics*, edited by M. Baldo (World Scientific, Singapore, 1999), Vol. 8, p. 121, and references therein.
- [5] H. Mütter, in *International Review of Nuclear Physics*, edited by M. Baldo (World Scientific, Singapore, 1999), Vol. 8, p. 170, and references therein.
- [6] M. Bender, P.-H. Heenen, and P.-G. Reinhard, *Rev. Mod. Phys.* **75**, 121 (2003), and references therein.
- [7] J.W. Negele and D. Vautherin, *Phys. Rev. C* **5**, 1472 (1972).
- [8] N. Kaiser, S. Fritsch, and W. Weise, *Nucl. Phys.* **A724**, 47 (2003), and references therein.
- [9] E. Epelbaum, Ulf-G. Meißner, W. Glöckle, and C. Elster, *Phys. Rev. C* **65**, 044001 (2002), and references therein.
- [10] P. Ring and P. Schuck, *The Nuclear Many-Body Problem* (Springer, Berlin, 1980), Chaps. 4 and 5.
- [11] N. Kaiser, R. Brockmann, and W. Weise, *Nucl. Phys.* **A625**, 758 (1997).
- [12] N. Kaiser, *Phys. Rev. C* **64**, 057001 (2001).
- [13] P. Büttiker and Ulf-G. Meißner, *Nucl. Phys.* **A668**, 97 (2000).
- [14] M. Beiner, H. Flocard, N. Van Giai, and P. Quentin, *Nucl. Phys.* **A238**, 29 (1975).
- [15] H. Krivine, J. Treiner, and O. Bohigas, *Nucl. Phys.* **A336**, 155 (1980).
- [16] J. Dobaczewski, H. Flocard, and J. Treiner, *Nucl. Phys.* **A422**, 103 (1984).
- [17] E. Chabanat, P. Bonche, P. Haensel, J. Meyer, and R. Schaeffer, *Nucl. Phys.* **A635**, 231 (1998).
- [18] F. Tondour, S. Goriely, J.M. Pearson, and M. Onsi, *Phys. Rev.*

- C **62**, 024308 (2000).
- [19] P.-G. Reinhard and H. Flocard, Nucl. Phys. **A584**, 467 (1995).
- [20] R. Machleidt, Phys. Rev. C **63**, 024001 (2001), and references therein.
- [21] V.G.J. Stoks, R.A.M. Klomp, C.P.F. Terheggen, and J.J. de Swart, Phys. Rev. C **49**, 2950 (1994).
- [22] R.B. Wiringa, V.G.J. Stoks, and R. Schiavilla, Phys. Rev. C **51**, 38 (1995).
- [23] S.K. Bogner, T.T.S. Kuo, and A. Schwenk, Phys. Rep. **386**, 1 (2003).
- [24] J.D. Holt, T.T.S. Kuo, G.E. Brown, and S.K. Bogner, Nucl. Phys. **A733**, 153 (2004).
- [25] J. Dobaczewski, work in progress and private communications.